Coherent scattering of undiluted Intralipid-20 % measured by critical-angle reflectometry

Ierotheos Katsoulis · draft of Nov 6, 2026

Self-published preprint, not peer-reviewed. Text and figures © 2026 Ierotheos Katsoulis, licensed CC BY 4.0; analysis code MIT-licensed. Measurements were made at the Electronic Devices and Materials Laboratory (EDML), Department of Electrical and Electronic Engineering, University of West Attica, during an MSc by Research supervised by Prof. Konstantinos Moutzouris (2020–2021). The full measurement dataset may be the property of EDML, UNIWA and is not disclosed; a representative sample is provided for verification and is not covered by the CC BY license. *Cite as:* I. Katsoulis, "Coherent scattering of undiluted Intralipid-20 % measured by critical-angle reflectometry," self-published preprint, November 2026.

Abstract

Undiluted Intralipid-20 % at 25 °C scatters about half as strongly as linear scaling of dilute measurements predicts. From critical-angle reflectance profiles, its scattering coefficient is 63 ± 15 mm^{-1} at 532 nm, 15 ± 5 mm^{-1} at 964 nm and 2.7 ± 1.9 mm^{-1} at 1551 nm. These values are 0.32–0.47 times the independent-scattering values and 0.84–1.05 times a recent dependent-scattering prediction.

The profiles were recorded with a commercial prism coupler and normalized to air. We fit the reflectance edge within 2° of the critical angle with a Fresnel profile for a complex effective index. The profile is blurred by the instrument's angular spread, measured on water, and sits on a floor of diffusely back-scattered light. The imaginary part k of the index gives the coherent extinction coefficient, $4\pi k/\lambda$. The same fit on water, whose k is known, shows a bias floor of 0.4–5 × 10^{-4} in k, which we subtract.

The scattering values depend on the reflectance model. The angle-dependent model of Dong et al. does not fit our data as published, because it has no term for diffuse light. With a diffuse floor it fits as well as ours and gives the same scattering at 964 and 1551 nm, but 1.6 times more at 532 nm. The refractive index is far less sensitive. Our fit and the corrected derivative method give n within 5 × 10^{-4} of each other, although their k values differ up to fourfold. For this turbid medium, critical-angle reflectometry gives n to about 10^{-3} but k only to tens of percent, and the derivative method's k should not be used.

1. Introduction

Intralipid-20 % is the most widely used scattering standard in tissue optics. Its scattering coefficient is usually measured on dilutions of 1 % or less and scaled linearly to the needed concentration [1, 2]. That scaling fails at high droplet volume fractions. The stock emulsion holds about 22.7 % oil by volume [1], and the positions of neighbouring droplets are correlated. Their scattered fields interfere, so the medium scatters less than the sum of isolated droplets would. This is dependent scattering. A recent model of it, built on a measured droplet-size distribution, predicts that independent scattering overestimates μ_s by more than 40 % already at half the stock concentration [3]. At full strength, direct tests exist only above about 1060 nm, the range where semi-empirical fits to integrating-sphere data are validated [3].

Critical-angle refractometry measures the reflectance at a prism–sample interface as a function of angle. In a turbid sample the reflected wave is the coherent part of the field, and its loss near the critical angle depends on the medium's extinction. Meeten and North described the principle for absorbing and turbid fluids [4, 5]. Morales-Luna and García-Valenzuela analysed its limits for colloids [6]. Calhoun, Bali and co-workers measured milk and Intralipid this way and extracted a complex effective index from the full profile of a divergent beam [7–10]. Closest to this work, Dong et al. fitted about 1000 points of the reflectance curve of a divergent, p-polarized 660 nm beam on undiluted Intralipid-20 %, with only n and k free. Using an empirical angle-dependent k in the total-reflection region, they found n = 1.36704 and k = 3.37 × 10^{-3} (64 mm^{-1}). With independent-scattering Mie theory they turned this into a mean droplet diameter of 0.32 μm, within 7 % of

dynamic light scattering [9]. The derivative method of Koutsoumpos et al. gives n and k from two features of the edge [11, 12]. Our companion papers showed that, with this kind of instrument, the angular spread of the beam biases both features [13, 14].

This paper uses the Intralipid scans of the companion turbid-media study [14] for a different quantity: the coherent extinction coefficient at three wavelengths. It adds four things to the work of Dong et al. and other critical-angle studies of Intralipid:

1. a fit of the whole edge that includes the instrument's angular spread, measured on water, and a floor for diffusely back-scattered light (Dong et al. fitted n and k only);
2. a bias floor for k measured on water, whose absorption is known, as a direct test of the method;
3. three wavelengths from 532 to 1551 nm and both polarizations, giving the spectral slope (Dong et al.: 660 nm, p-polarization);
4. a comparison with independent and dependent scattering for the stock emulsion (Dong et al. assumed independent scattering).

2. Theory

Coherent wave and effective index. In a turbid medium the mean (coherent) field propagates as a plane wave in a homogeneous medium with complex effective index m = n + ik. Its intensity decays as exp(−μ_{ext} z), with

$$\mu_{\mathrm{ext}} = \frac{4\pi k}{\lambda} = \mu_s + \mu_a$$

where λ is the wavelength in air (the index is measured relative to air). At the prism–sample interface the coherent reflectance $R_{coh}(\theta)$ follows the Fresnel equations for m. Above the critical angle the transmitted coherent wave is evanescent. Its extinction removes energy, so R_{coh} drops below 1 and the edge at θ_c rounds off. The rounding width scales with k.

This description holds when the effective medium is local, that is, when the droplets are small compared with the wavelength and the decay depth. Intralipid droplets range from about 60 nm to 2 μm, with most of the volume below 600 nm [1]. We treat m as an effective parameter and discuss the limits in Section 6.

Diffuse floor. Below θ_c, light enters the sample, is scattered many times and partly returns into the prism. The detector collects the part that falls within its acceptance cone. If a fraction β of the coherent loss returns this way, the measured reflectance is

$$R(\theta) = R_{\mathrm{coh}} + \beta\,(1 - R_{\mathrm{coh}}) = a + b\,R_{\mathrm{coh}}(\theta + \delta\theta;\, n, k, \sigma)$$

with a = β and b = 1 − β. We leave b free, because it also absorbs residual differences in laser power and alignment between the sample scan and its air scan. Here δθ is the rotation-direction offset and σ the Gaussian angular spread of the beam, both taken from water [13]. The level of R at θ_c depends on a and b. The shape of the knee depends on k. The derivative method reads k from the level [11], so diffuse light biases it. A fit of the shape avoids this.

Expected scattering. For independent scattering we use the fit of Attendu et al. [3] to Mie calculations over the measured size distribution, scaled to the stock volume fraction φ = 0.227:

$$\mu_s^{\mathrm{IS}}(\lambda) = 108.2\,x^{-2.516 - 0.4036\,\log_{10} x}\ \mathrm{mm}^{-1}, \qquad x = \lambda/600\ \mathrm{nm}$$

The independent fit of Shahsavari et al. [1], 163.7 (λ/500 nm)$^{-2.546}$ mm^{-1}, agrees with it within 8 % at our three wavelengths. For dependent scattering we multiply by the packing factor of the semi-empirical relation used in [3]:

$$\mu_s^{\mathrm{DS}} = \mu_s^{\mathrm{IS}}\,\frac{(1-\phi)^{p+1}}{\left[1+\phi\,(p-1)\right]^{p-1}}, \qquad p(\lambda) = 1.207 + 0.3078\,\frac{\lambda}{600\ \mathrm{nm}}$$

We reconstructed this form from the paper's text. It reproduces the paper's statement that independent scattering overestimates μ_s by more than 40 % at 800 nm and $\varphi = 0.114$: the formula gives 43 %. At $\varphi = 0.227$ the factor is 0.50 at 532 nm, 0.45 at 964 nm and 0.38 at 1551 nm.

3. Samples, instrument and data

All scans were recorded in 2020–21 at the Electronic Devices and Materials Laboratory (EDML), University of West Attica, on a Metricon 2010/M prism coupler [15] used as a critical-angle refractometer. The sample cell was held at 25 °C. A rotary table scans the internal angle in steps of about 0.0036°. A photodetector records the reflected intensity. Four lasers were used: 532, 964 and 1551 nm for Intralipid, and additionally 633 nm for water. The prism indices at 25 °C are 1.9775 (532 nm), 1.9450 (964 nm) and 1.9340 (1551 nm). The prism material is not documented.

Intralipid. The sample was undiluted Intralipid-20 % (20 % soybean oil, about 22.7 % by volume [1]). Each Intralipid scan was divided by an air scan at the same wavelength and polarization. Air is totally reflected over the whole range, so $R(\theta) = I_{\mathrm{sample}}/I_{\mathrm{air}}$ is the absolute reflectance up to a scale factor near 1. Two protocols were used. In the slow protocol each sample scan has its own air scan. In the fast protocol several sample scans share one air scan taken just before them. All Intralipid scans were taken in rotation direction R.

Wavelength	Slow protocol, TE / TM	Fast protocol, TE / TM	Total
532 nm	5 / 5	–	10
964 nm	6 / 6	5 / 4	21
1551 nm	5 / 5	5 / 5	20

The files for the 532 nm Intralipid scans carry an internal name with "633". Their refractive index, 1.3691, and the dispersion across the three wavelengths show they were taken at 532 nm [14].

Water. 194 water scans at 25 °C (TE and TM, both rotation directions, 532/633/964/1551 nm) come from the companion water study [13, 16]. They give the instrument parameters used here: the angular spread σ (0.021° at 532 nm, 0.014° at 633 nm, 0.025° at 964 nm, 0.024° at 1551 nm) and the rotation-direction offset. We also use them in Section 4.3 to measure the bias floor of the k fit. The water scans have no air reference, so their scale factor b also absorbs the angular response of source and detector.

4. Analysis

4.1 Edge-shape fit

For each Intralipid scan we take θ_c from the derivative maximum of $R(\theta)$ [14]. We fit $R(\theta)$ between $\theta_c - 2°$ and $\theta_c + 2°$ with the model of Section 2 (four free parameters: n, $\log_{10}$ k, a, b). The spread σ and the offset δθ are fixed at the water values for that wavelength. The model is the Fresnel reflectance convolved with a Gaussian of standard deviation σ on a 0.0002° grid. The fit is a bounded least-squares fit started from four values of k ($10^{-3.5}$ to 10^{-2}), keeping the best. For comparison we repeat each fit with a = 0, which is a Fresnel profile with free scale only.

4.2 Robustness

We refit the slow-protocol scans with four variants: windows of ±1° and ±3°, an asymmetric window from −1° to +2.5°, and a floor with a linear slope in θ. Half the range of the variant medians is the model uncertainty of

k. Raising σ by its uncertainty changes k by less than 1 % at 532 and 964 nm and by 5 % at 1551 nm, which is negligible against the other terms.

4.3 Bias floor measured on water

Water's extinction is known, from 1.5×10^{-9} at 532 nm to 1.3×10^{-4} at 1551 nm. We ran the same fit on the 194 water scans. Any k above the true value is a bias of the method at that wavelength and polarization.

λ (nm)	k fitted, TE (10^{-4})	k fitted, TM (10^{-4})	k true (10^{-4})	Floor, TE (10^{-4})	Floor, TM (10^{-4})
532	5.4	1.2	0.00	5.4	1.2
633	1.6	0.09	0.00	1.6	0.09
964	2.1	0.45	0.03	2.1	0.42
1551	5.0	3.2	1.3	3.7	1.9

The floor is larger in TE than in TM at every wavelength. This matches the polarization dependence of the blur artifact found for the derivative method [13]. With a sloped floor the water k at 532 and 633 nm drops below 10^{-5}, but at 1551 nm it stays at 3.0–3.4 × 10^{-4}. We take the values in the table, which are the larger, as the floor and give them a 50 % uncertainty plus half the TE–TM difference. The floor is subtracted from each Intralipid median per wavelength and polarization. The corrected TE and TM values are then averaged.

4.4 From k to μ_s

The extinction is $\mu_{ext} = 4\pi k/\lambda$. Absorption by the aqueous phase is $\mu_a = 4\pi k_w(1 - \varphi)/\lambda$, which is 0.81 mm^{-1} at 1551 nm, 0.03 mm^{-1} at 964 nm and negligible at 532 nm. We subtract it to get μ_s. Absorption by the soybean oil is neglected.

4.5 Uncertainty budget

Term, k (10^{-4})	532 nm	964 nm	1551 nm
Scan-to-scan (robust standard error)	1.5	1.0	0.3
Fit model (Section 4.2)	5.0	3.7	0.2
Bias floor (Section 4.3)	3.7	1.5	2.3
Combined	6.4	4.1	2.4
Combined, as μ_s (mm^{-1})	15.1	5.4	1.9

At 532 and 964 nm the choice of fit model dominates. At 1551 nm the bias floor dominates, and it is comparable to the Intralipid signal itself.

5. Results

5.1 The diffuse floor is needed, and it falls with wavelength

Adding the diffuse floor lowers the median fit residual from 0.053 to 0.013 at 532 nm, from 0.031 to 0.005 at 964 nm and from 0.025 to 0.003 at 1551 nm (Fig. 1). Without the floor, the fit can match the raised reflectance below θ_c only by making the whole edge very broad, which drives k to 1.6×10^{-2} at 532 nm. The fitted floor a is 0.24 at 532 nm, 0.14 at 964 nm and 0.06 at 1551 nm. This is the expected order: the medium scatters less at longer wavelengths, and at 1551 nm water absorption also removes multiply scattered light before it returns. The real part of the index is unchanged: the edge-shape fit gives n = 1.3686, 1.3592 and 1.3517, within 5 × 10^{-4} of the values in [14].

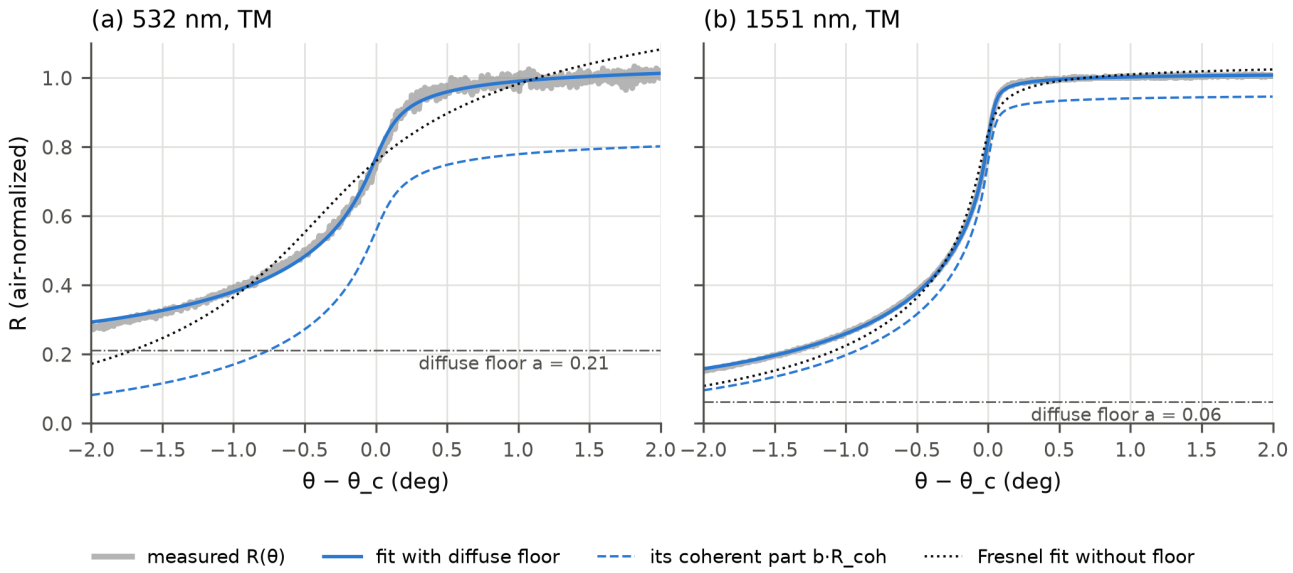


Fig. 1. Air-normalized reflectance of undiluted Intralipid-20 % (grey, one TM scan each) at (a) 532 nm and (b) 1551 nm. Blue: fit with diffuse floor; dashed blue: its coherent part $b \cdot R_{coh}$; dotted black: Fresnel fit without floor. The dash-dot line marks the fitted floor a.

5.2 Extinction and scattering coefficients

The derivative method, which reads k from the level of the edge, gives 4–7 × 10^{-4} at all three wavelengths. The edge-shape fit gives 3.0 × 10^{-3} at 532 nm, falling to 7.6 × 10^{-4} at 1551 nm. The table lists the edge-shape results, the bias floor from Section 4.3, and the resulting scattering coefficients.

λ (nm)	k, TE / TM (10^{-4})	Floor-corrected k, TE / TM (10^{-4})	μ_s (mm^{-1})	μ_s^{IS} (mm^{-1})	μ_s^{DS} (mm^{-1})	μ_s / μ_s^{DS}	μ_s / μ_s^{IS}
532	30.3 / 29.4	24.9 / 28.2	63 ± 15	146	73	0.85 ± 0.21	0.43 ± 0.10
964	11.6 / 13.8	9.5 / 13.4	15 ± 5	31.6	14.2	1.05 ± 0.38	0.47 ± 0.17
1551	7.9 / 6.3	4.2 / 4.5	2.7 ± 1.9	8.5	3.2	0.84 ± 0.60	0.32 ± 0.22

At every wavelength the measured μ_s agrees with the dependent-scattering prediction within its uncertainty (Fig. 2). It lies below the independent-scattering value by 5.5 standard uncertainties at 532 nm and by 3.1 at both 964 and 1551 nm. Before the floor correction the ratios to the dependent-scattering value are 0.96, 1.21 and 1.67. The correction matters only at 1551 nm. There it also brings TE and TM into agreement: 4.2 and 4.5 × 10^{-4} after correction, against 7.9 and 6.3 × 10^{-4} before.

Between 532 and 964 nm the measured μ_s falls as $\lambda^{-2.4}$, and the dependent-scattering prediction as $\lambda^{-2.8}$. The 1551 nm point is too uncertain to constrain the slope further.

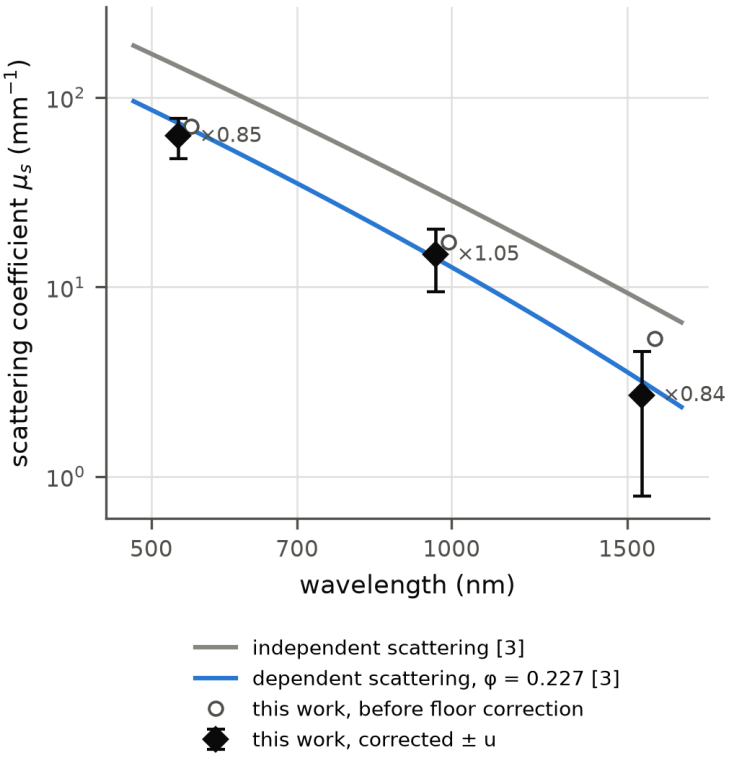


Fig. 2. Scattering coefficient of undiluted Intralipid-20 % at 25 °C. Filled diamonds: this work after bias-floor correction, with combined standard uncertainty; open circles: before correction. Grey line: independent scattering [3]; blue line: dependent scattering at φ = 0.227 (Section 2). Labels give the ratio to the dependent-scattering value.

5.3 Protocols and polarizations

At 1551 nm the slow and fast protocols agree within 6 % (k = 7.6 and 7.2 × 10^{-4}). At 964 nm they differ: 1.8 × 10^{-3} (slow) against 1.2 × 10^{-3} (fast). Three slow scans at 964 nm have much broader edges (k = 2.9–8.2 × 10^{-3}), which raises the slow median. The fast scans were taken in quick succession and are tightly grouped (within ±3 % per polarization). The 964 nm uncertainty in the table includes this difference through the fit-model term. TE and TM agree within 25 % before the floor correction at all wavelengths.

5.4 Model dependence: the angle-dependent model of Dong et al.

We fitted all 51 scans with the model of Dong et al. [9]. Above a transition angle θ_t their absorption is multiplied by $\kappa(\theta) = 1/(4\pi\, n_p\, \mathrm{Im}\, w)$, with $w = \sqrt{(m^2/n_p^2 - \sin^2\theta)}$. The free parameters are n, k and θ_t.

As published, the model fits our data poorly (Fig. 3). Over the whole scan its residual is 0.03–0.10, against 0.002–0.025 for our model. It predicts R falling almost to zero far below θ_c, where our data stay at 0.05–0.15. To compensate, n moves by up to 0.03 and the TE and TM values of k differ by up to sixfold.

With our diffuse floor added (a + b times the blurred model), Dong's model fits as well as ours. Its residual is 0–25 % lower, with one more parameter. On water it returns the same bias floor as our fit, within 15 %. The data therefore cannot tell a constant k from Dong's angle-dependent one, but the two give different values in the ±2° window:

λ (nm)	k, our model (10^{-4})	k, Dong + floor (10^{-4})	μ_s, our model (mm^{-1})	μ_s, Dong + floor (mm^{-1})	μ_s^{DS} (mm^{-1})	μ_s^{IS} (mm^{-1})
532	30	46	63	101	73	146
964	13	15	15	17.5	14.2	31.6
1551	7.6	6.3	2.7	2.5	3.2	8.5

k is the median over TE and TM before the bias-floor correction; μ_s is after it, with each model's own water floor. At 964 and 1551 nm the two models agree within their uncertainties, and both exclude independent scattering. At 532 nm Dong's model lands halfway between the two predictions. There the choice of model is the largest uncertainty, and that point alone no longer separates dependent from independent scattering.

Fitting the whole scan, as Dong et al. did, is less reliable on our data with either model. At 532 nm, n moves by 0.002–0.01 and k roughly doubles, because the diffuse light far below the edge is not constant. We therefore keep the ±2° window.

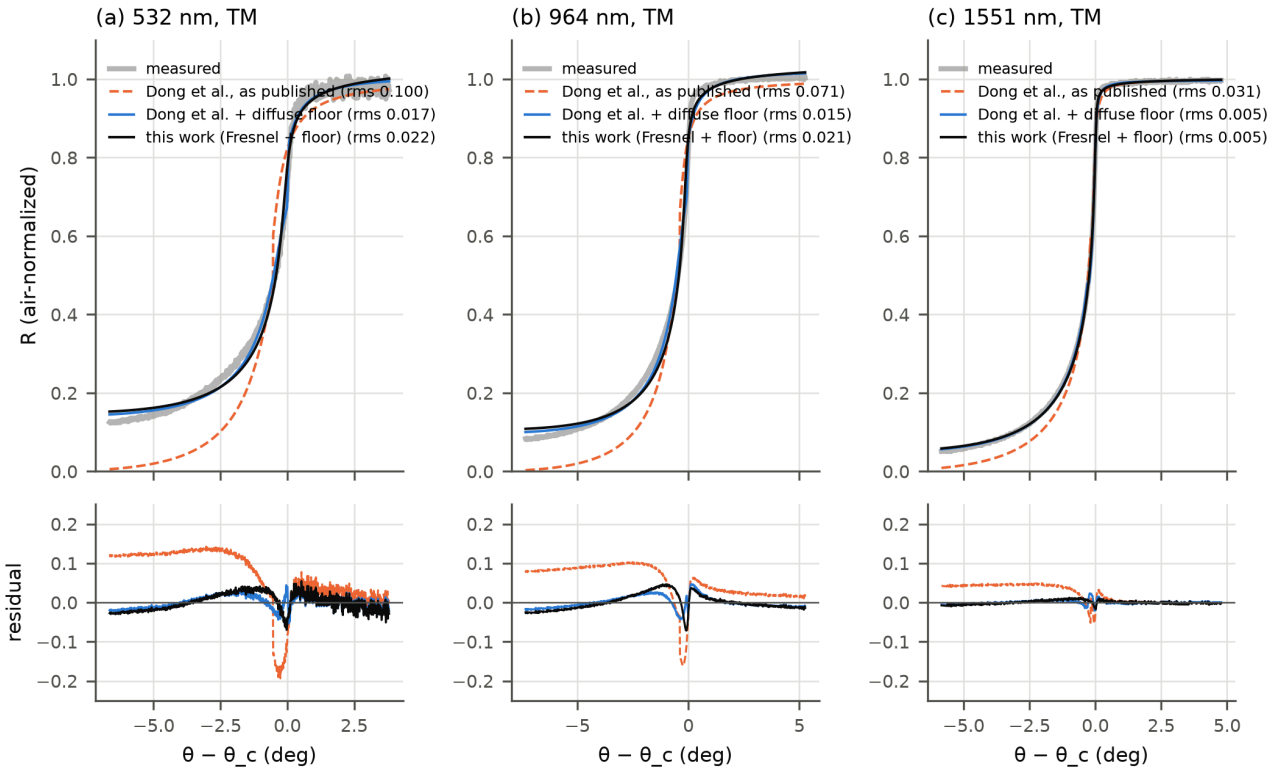


Fig. 3. Whole-scan fits of one TM scan at (a) 532, (b) 964 and (c) 1551 nm: the model of Dong et al. as published (dashed orange), the same model plus a diffuse floor (blue), and our model (black). Residuals below; the rms residual of each fit is in the legend.

6. Discussion

What the data show. Scaling dilute measurements linearly to the stock emulsion overestimates its scattering about twofold at 964 and 1551 nm, whichever reflectance model is used. The dependent-scattering model [3] accounts for that factor. At 532 nm the conclusion depends on the model (Section 5.4). At $\varphi = 0.227$ the semi-empirical relations behind the model are validated only above about 1060 nm [3], so our 532 and 964 nm points lie outside that range. We chose the fit window, the floor and the corrections after seeing the data. We therefore read the agreement with dependent scattering as consistency, not as a precise test.

Coherent extinction is not exactly bulk μ_s. Three effects could separate the two, and we have not modelled them.

- *Depth probed.* Just above θ_c the coherent field decays into the sample over a depth that falls from many micrometres at θ_c to about 0.5 µm at $\theta_c + 0.5°$ (at 532 nm). That is comparable to the largest droplets. Droplet centres cannot come closer to the prism than one radius, so the layer next to the wall is depleted. Morales-Luna and García-Valenzuela showed that such non-local effects limit critical-angle measurements of colloids [6].

- *Forward scattering.* Intralipid scatters strongly forward (g ≈ 0.78 at 532 nm [1]). Light scattered at small angles stays close to the specular direction and may be counted partly as coherent. This would lower the apparent extinction, in the same direction as dependent scattering.
- *Shape of the diffuse floor.* We model the floor as proportional to the coherent loss. Its true angular shape depends on the detector's acceptance and on multiple scattering. The sloped-floor variant changes k by up to 20 %, and that is included in the uncertainty.

The agreement at 964 and 1551 nm suggests these effects are smaller than our uncertainties there, but it does not prove it. A test on dilutions, where independent scattering is known to hold, would separate the method from the physics. The data set contains no dilutions.

n is robust, k is not. The corrected derivative method [14] and our edge-shape fit give n within 5×10^{-4} of each other at all three wavelengths, although their k values differ up to fourfold. Dong's model with a floor gives n lower by 2×10^{-3} at 532 and 964 nm and the same value at 1551 nm. The derivative method reads k from the height of the reflectance at θ_c, which diffuse light raises. Its k for Intralipid ($4–7 \times 10^{-4}$) is 1.2–4 times below the edge-shape value. Its n comes mainly from the position of the edge and is barely affected. For turbid samples the derivative method is therefore a good tool for n and a poor one for k. The spread between models raises the n uncertainty at 532 and 964 nm from $\pm 8 \times 10^{-4}$ to about $\pm 2 \times 10^{-3}$, as now stated in [14].

1551 nm is the weakest point. There the Intralipid k is 7.6×10^{-4}. Water absorption accounts for 1.0×10^{-4} of it and the bias floor for $2–4 \times 10^{-4}$. The scattering part left after both subtractions is 3.3×10^{-4} with an uncertainty of 2.4×10^{-4}. The point agrees with dependent scattering and lies 3.1 standard uncertainties below independent scattering, but alone it would not separate the two well.

Concentration and sample age. The sample was Intralipid-20 %; a 2021 lab note that gives "25 % fat" is in error. The concentration of Intralipid-20 % varies by 19 % on average between batches [1]. The age and storage of the sample are not recorded, and droplets in an opened emulsion can grow with time. A 10–20 % error in φ changes the dependent-scattering prediction by less than that, because the packing factor partly offsets the linear term. It cannot account for the twofold difference from independent scattering.

Comparison with Dong et al. A power-law interpolation of our values gives $\mu_s = 37 \pm 8$ mm^{-1} at their wavelength of 660 nm. The dependent-scattering prediction there is 41 mm^{-1} and the independent one 85 mm^{-1}. From one data set, Dong et al. found 64 mm^{-1} with their angle-dependent model and 25 mm^{-1} with plain Fresnel theory, at similar fit quality [9]. Applied to our scans (Section 5.4), their model as published does not fit. With a floor it fits, but it gives 1.6 times our scattering at 532 nm. Both results say the same thing: k from a reflectance fit depends strongly on the model, which is why we test every model on water. Their particle size assumed independent scattering, which is the assumption our data test at φ = 0.227. Their real index, 1.36704, lies inside the range 1.363–1.368 that dispersion fits through our three wavelengths give at 660 nm [14]. They also noted that the droplet density in a surface layer one diameter thick may differ from the bulk [9], the effect listed above under depth probed.

7. Conclusions

1. With instrument corrections, critical-angle reflectometry gives the refractive index of undiluted Intralipid-20 % to about 10^{-3}. The result barely depends on how k is modelled.
2. The extinction coefficient can be read from the edge shape once diffusely back-scattered light is modelled. It depends on the reflectance model by up to 1.6 times at 532 nm, so it is good to tens of percent, not better.
3. Undiluted Intralipid-20 % scatters about half as strongly as linear scaling of dilute data predicts. With both models we find 15–18 mm^{-1} at 964 nm and 2.5–2.7 mm^{-1} at 1551 nm, consistent with dependent scattering at φ = 0.227. At 532 nm the value is 63–101 mm^{-1}, depending on the model.

4. The derivative method's k for this emulsion ($4–7 \times 10^{-4}$) is biased low by diffusely back-scattered light, by up to fourfold, and should not be read as an extinction coefficient. Its n is not affected.
5. A bias floor measured on water ($0.4–5 \times 10^{-4}$ in k, larger in TE) sets the detection limit for k on this instrument.
6. A more precise k needs samples of known extinction, such as absorbing dyes, dilution series or monodisperse spheres. This data set contains none.

Known open issues

- Check the reconstructed dependent-scattering formula against the typeset equations of [3] and the original semi-empirical relation it cites.
- Replace the empirical diffuse floor and the angle factor of Dong et al. with a coherent-reflection model for polydisperse spheres near a wall, to resolve the model dependence at 532 nm.
- Decide whether the 532 and 633 nm water floors should come from the sloped or unsloped fit.
- Test the method on samples of known extinction (absorbing dyes, Intralipid dilutions, monodisperse spheres).

Data and code

A representative sample of the raw scans is provided with this release for verification (`data_sample/`, 16 files: water at 964 and 1551 nm in both polarizations and rotation directions, Intralipid at 1551 nm and cream at 633 nm with their air references). The full dataset (252 water scans, and 115 Intralipid and cream scans with their air references) was recorded at EDML, UNIWA; it may be the property of the laboratory and is not disclosed. The complete analysis code is included (`code/`): it reproduces every number in this paper when run on the full dataset, and processes the sample files individually.

Measurements: Ierotheos Katsoulis, Electronic Devices and Materials Laboratory (EDML), University of West Attica, during an MSc by Research supervised by Prof. Konstantinos Moutzouris. Analysis and text: Ierotheos Katsoulis, 2026.

References

1. M. Shahsavari, M. Kuiper, M. Engelaer, M. Poinsinet de Sivry-Houle, T. G. van Leeuwen, E. van der Pol, "Particle size distribution and concentration of Intralipid® 20%," J. Biomed. Opt. 31, 015001 (2026). PMC12828180
2. L. Spinelli et al., "Determination of reference values for optical properties of liquid phantoms based on Intralipid and India ink," Biomed. Opt. Express 5, 2037–2053 (2014). PMC4102347
3. X. Attendu, M. Poinsinet de Sivry-Houle, M. Shahsavari, D. J. Faber, E. van der Pol, T. G. van Leeuwen, "Scattering properties of Intralipid modeled using dependent scattering theory," J. Biomed. Opt. 31, 085003 (2026). PMC13521324
4. G. H. Meeten, A. N. North, "Refractive index measurement of absorbing and turbid fluids by reflection near the critical angle," Meas. Sci. Technol. 6, 214–221 (1995). doi:10.1088/0957-0233/6/2/014
5. G. H. Meeten, "Refractive index errors in the critical-angle and the Brewster-angle methods applied to absorbing and heterogeneous materials," Meas. Sci. Technol. 8, 728–733 (1997). doi:10.1088/0957-0233/8/7/006
6. G. Morales-Luna, A. García-Valenzuela, "Viability and fundamental limits of critical-angle refractometry of turbid colloids," Meas. Sci. Technol. 28, 125203 (2017). doi:10.1088/1361-6501/aa8fbe
7. W. R. Calhoun, H. Maeta, A. Combs, L. M. Bali, S. Bali, "Measurement of the refractive index of highly turbid media," Opt. Lett. 35, 1224 (2010). doi:10.1364/OL.35.001224
8. W. R. Calhoun, H. Maeta, S. Roy, L. M. Bali, S. Bali, "Sensitive real-time measurement of the refractive index and attenuation coefficient of milk and milk-cream mixtures," J. Dairy Sci. 93, 3497–3504 (2010). doi:10.3168/jds.2010-3045
9. M. L. Dong, K. G. Goyal, B. W. Worth, S. S. Makkar, W. R. Calhoun, L. M. Bali, S. Bali, "Accurate in situ measurement of complex refractive index and particle size in intralipid emulsions," J. Biomed. Opt. 18, 087003 (2013). doi:10.1117/1.JBO.18.8.087003
10. K. G. Goyal, M. L. Dong, V. M. Nguemaha, B. W. Worth, P. T. Judge, W. R. Calhoun, L. M. Bali, S. Bali, "Empirical model of total internal reflection from highly turbid media," Opt. Lett. 38, 4888 (2013). doi:10.1364/OL.38.004888
11. S. Koutsoumpos, P. Giannios, I. Stavrakas, K. Moutzouris, "The derivative method of critical-angle refractometry for attenuating media," J. Opt. 22, 075601 (2020). doi:10.1088/2040-8986/ab8286

12. S. Koutsoumpos, P. Giannios, K. Moutzouris, "Critical angle refractometry for lossy media with a priori known extinction coefficient," Physics 3, 569–578 (2021). doi:10.3390/physics3030036
13. I. Katsoulis, "Apparent birefringence in critical-angle refractometry: a polarization bias of the derivative method" (2026). axiosyn.com/optics
14. I. Katsoulis, "Complex refractive index of Intralipid and milk cream by instrument-corrected critical-angle refractometry" (2026). axiosyn.com/optics
15. Metricon Corporation, Model 2010/M prism coupler. metricon.com
16. I. Katsoulis, "Polarization-resolved critical-angle refractometry of liquid water (532–1551 nm, 25–80 °C)" (2026). axiosyn.com/optics